Optimization and Durability of Reversible Solid Oxide Cells

Sun, X.; Sudireddy, B. R.; Tong, X.; Chen, M.; Brodersen, K.; Hauch, A.

Published in:
ECS Transactions

Link to article, DOI:
10.1149/09101.2631ecst

Publication date:
2019

Document Version
Publisher's PDF, also known as Version of record

ECS Transactions, 91 (1) 2631-2639 (2019)
10.1149/09101.2631ecst ©The Electrochemical Society

Optimization and Durability of Reversible Solid Oxide Cells

X. Sun [a], B. R. Sudireddy [a], X. Tong [a], M. Chen[a], K. Brodersen [a], and A. Hauch [a]

[a] Department of Energy Conversion and Storage, Technical University of Denmark, Roskilde DK-4000, Denmark

Reversible solid oxide cells (rSOCs) hold a considerable potential to play a very important role in the future energy system. The present work focuses on understanding the effect of initial cell performance, duration of the operation when cycling between SOFC and SOEC modes, current density and temperature on the durability of rSOCs. Two different cell designs are developed and their performance in reversible operation was evaluated. Type I is Ni-yttria stabilized zirconia (Ni-YSZ) fuel electrode supported planar SOCs, with a LSC-CGO ($La_{0.6}Sr_{0.4}CoO_{3-\delta}$-$Ce_{0.9}Gd_{0.1}O_{2-\delta}$) composite oxygen electrode, Type II is the same fuel-electrode supported half-cell with CGO oxygen electrode backbone infiltrated with LSC nano-electrocatalysts. Comparable degradation rates of below 5-10%/1000 hours were achieved for Type I cells operated at ±0.5 A/cm^2, or for Type II cells operated at ±1.25 A/cm^2. The electrochemical performance and durability of both cell types are compared and the observed degradation behavior is discussed.

Introduction

The integration of high amount of fluctuating renewable energy such as wind or solar energy into the existing energy grid requires efficient and cost competitive energy conversion and storage technologies to balance the energy production and consumption. Reversible solid oxide cells (rSOCs) hold the potential to play a very important role in the future energy system. rSOCs can be operated both as fuel cell and electrolysis cell. When operated as a solid oxide electrolysis cell (SOEC), electrical energy can be converted to chemical energy and stored as H_2 or synthesis gas (syngas, CO + H_2) via high temperature electrolysis of steam or co-electrolysis of steam and CO_2 (1–3). H_2 and syngas can be further processed to a variety of synthetic fuels, which may be stored and later reconverted into electricity using the same rSOC, but operated as a solid oxide fuel cell (SOFC) or used as fuel for transportation. The capability of such a reversible operation makes rSOC very attractive for grid balancing or decentralized grid independent energy source application. System modelling results showed that a round trip efficiency (power-to-gas-to-power) of up to 80% could be achieved by combing pressurized operation and storing the electricity as chemical bound energy in CH_4 (1). rSOC system with 50 kW SOFC and 120 kW SOEC has been demonstrated (5). However, long-term durability of rSOC is still a challenge for large-scale commercialization of this technology. Extensive studies have been carried out on both SOFC and SOEC cells and

stacks (1,6) , but only few studies have been reported on the rSOCs (5,7). It has been reported that the degradation of SOC is strongly influenced by the different operation period of electrolysis mode and different oxygen electrode materials (7,8). It is expected that for grid balancing purpose, the operation time in either fuel cell mode or electrolysis mode will be depended on the electricity market price, and with the increase in implementation renewable electricity sources, operation period in SOFC mode may be shorter than the one in SOEC mode. It is therefore necessary to understand the degradation of the SOC when operated in different reversible conditions, such as cycle time, current densities etc. and explore different oxygen electrode materials/configurations that potentially lower the SOC degradation.

The present work focuses on understanding the influence of initial cell performance, duration of the operation in SOFC and SOEC modes, current density and temperature on the durability of rSOCs. Furthermore, the improvement of the rSOC's performance by infiltration of nano-electrocatalysts in a CGO backbone is explored. The performance and durability are compared for the two types of cells and the degradation mechanisms are discussed.

Experimental

Sample preparation

Two different types of cells are developed. Type I is Ni-yttria stabilized zirconia (Ni-YSZ) fuel electrode supported planar SOCs, with LSC-CGO ($La_{0.6}Sr_{0.4}CoO_{3-\delta}$-$Ce_{0.9}Gd_{0.1}O_{2-\delta}$) composite oxygen electrode that was produced at DTU Energy (9). The cell consists of a ~10 µm thick Ni-8YSZ fuel electrode with a ~300 µm thick Ni-3YSZ support layer, a ~10 µm thick YSZ electrolyte, a ~6 µm thick CGO diffusion barrier layer and a ~30 µm thick LSC-CGO oxygen electrode and a ~30 µm thick LSC contact layer. Type II cells consist of the same fuel-electrode, support layer, electrolyte layer, a ~6 µm thick CGO diffusion barrier layer, a CGO porous backbone infiltrated with LSC nano-electrocatalysts and a ~30 µm thick LSC contact layer. The support layer, fuel electrode, electrolyte and CGO diffusion barrier layer, in the case of type I cells, as well as the porous CGO backbone layer in the case of type II cells, were fabricated using tape casting. The LSC-CGO oxygen electrode for Type I cells and LSC contact layer for both types were made by screen printing. Integration of the oxygen electrode electrocatalyst was performed by infiltrating the aqueous solutions of respective metal nitrates of La, Sr and Co in appropriate quantities. The infiltration cycles were repeated until required loading of LSC was achieved. After the infiltration the cells were treated at 500 ^{o}C for 30 minutes to decompose the nitrates. The cell dimensions of both Type I and Type II cells are 53×53 mm^2 with an active area (oxygen electrode area) of 40×40 mm^2.

Electrochemical characterization

For testing, the cell was mounted in an alumina cell test house. Ni and Au meshes were used for current collector for the fuel and oxygen electrode side, respectively. An Au frame was used for sealing the fuel electrode compartment and no sealing was applied for the oxygen electrode side. At startup, a 4 kg of weight load was added on the top of the cell house. The cells were heated to 850 ˚C with a ramp rate of 1 ˚C/min, and 20 L/h

N_2 was supplied to the fuel electrode compartment and 20 L/h Air was supplied to the oxygen electrode. The NiO in the cellwas then reduced in 20 L/h of 5% H_2 + N_2 for 2 hours then 24 L/h H_2 + 4% H_2O for 1 hour.

The initial performance characterization on all tested cells was carried out by measuring DC polarization (i-V) curves and AC electrochemical impedance spectra (EIS) at 850, 800, 750 and 700°C. Gas shift impedance characterizations were performed by varying gas atmospheres at the Ni-YSZ fuel electrode (by changing the H_2O concentration in H_2 + H_2O mixture) and the at the LSC-CGO oxygen electrode (by switching between air and O_2) respectively. The impedance spectra were measured at zero current using a Solartron 1255B frequency analyzer and an external shunt connected in series with the cell. The spectra were recorded from 96850 to 0.08 Hz with 12 points per decade and were corrected using the short circuit impedance response of the test setup. From the impedance spectra, the ohmic (serial) resistance (R_s) was taken as the value of the real part of the impedance measured at 96850 Hz and the polarization resistance (R_p) was taken as the difference in the real part of the impedance at 96850 Hz and 0.08 Hz. The total area specific resistance of a cell was calculated as the sum of the real part of the impedance (R_s + R_p).

Durability test was carried out after the initial performance characterization. The test procedure was aligned with the test program published by the European project SOCTESQA (10). The test procedure starts with a short period of 5 days (120 hours) SOFC and 5 days (120 hours) of SOEC "pre-conditioning" tests prior to the reversible operation. The pre-conditioning test were carried out at 0.5 A/cm^2 (SOFC mode) or -0.5 A/cm^2 (SOEC) mode with 50% H_2 + N_2 (SOFC mode) or 20% H_2 + H_2O (SOEC mode) supplied to the fuel electrode compartment and Air to the oxygen electrode compartment. The reactant conversion calculated based Faraday law in both modes is 52%. The reversible operation was then performed with 50% H_2 + N_2 supplied to the fuel electrode in SOFC mode and 20% H_2 + H_2O supplied to the fuel electrode in SOEC mode. iV and EIS measurements were carried out before and after each mode to check the performance. Table I presents the test conditions.

TABLE I. List of tested cells and test conditions.

Cell number	Cell type	Temperature, ˚C	Reversible current density, A/cm^2	SOFC/SOEC period, hour
Cell A	I	750	±0.5	3/20
Cell B	I	750	±0.5	3/8
Cell C	I	700	±0.5	3/20
Cell D	II	700	±0.5	3/20
Cell E	II	700	±1.25	3/20

Results and Discussion

Effect of SOFC/SOEC operation time

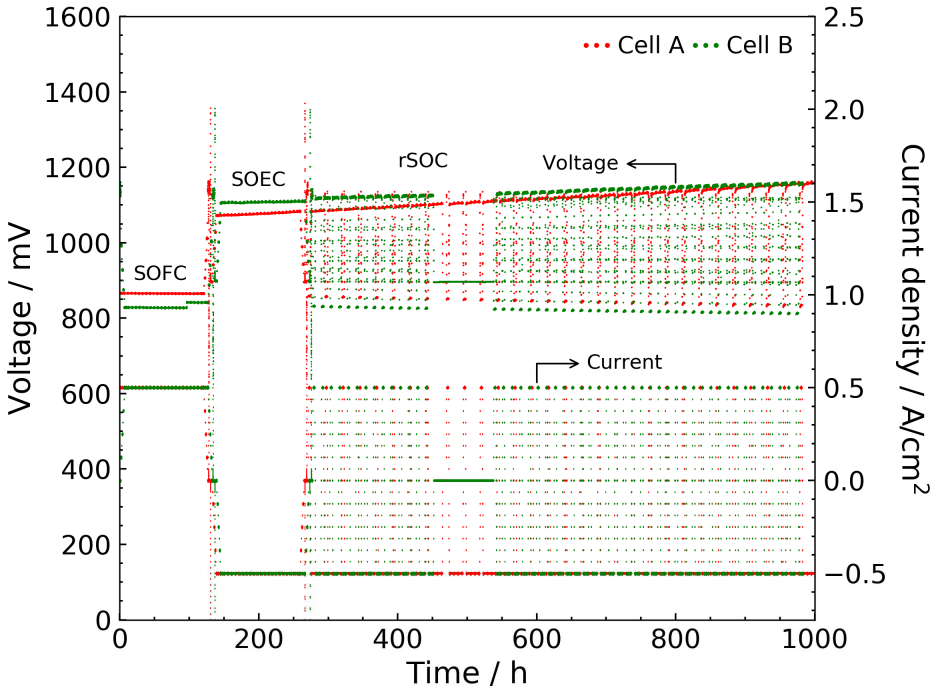

Figure 1. Effect of cycle time on the degradation of rSOC. During reversible operation periods, Cell A was operated for 3 hours in SOFC and 20 hours in SOEC per cycle, while Cell B was operated for 3 hours in SOFC and 8 hours of SOEC per cycle.

The effect of changing SOFC/SOEC operation time on the degradation of rSOC is presented in Figure 1. Where both cells were operated for 120 hours in SOFC mode and 120 hours in SOEC mode before shifted to reversible operation. During reversible operation, Cell A was operated 1 cycle per day with 20 hours in SOEC and then 3 hours of SOFC and cell B was operated 2 cycles per day with 8 hours of SOEC and 3 hours SOFC. It has to be noted that for the first 100 hours of SOFC operation of Cell B, the fuel gas composition was 24% H_2 + Ar instead of 50% H_2 + 50% N_2, which caused a lower cell voltage mainly caused by higher conversion as compared with the last 20 hours operation in 50% H_2 +50% N_2. It can be seen from the cell voltage that during pre-conditioning in constant operation mode, Cell B showed slightly lower performance but better durability in comparison with Cell A.

TABLE II. Cell voltage degradation rate in different operation modes for cell A (3 hours SOFC and 20 hours SOEC per cycle) and Cell B (3 hours SOFC and 8 hours SOEC per cycle)

Degradation rate, %/1000 h	**Constant operation**		**Reversible operation**	
	SOFC mode	**SOEC mode**	**SOFC mode**	**SOEC mode**
Cell A	0.67	8.2	3.8	10
Cell B	0	3.3	3.2	5

Table II presents the degradation rates of the two tested cells calculated based on cell voltage and the operation time. It is worth noting that the operating time was only 120 hours for the pre-conditioning tests and therefore the derived degradation rates in such a short time will not be as representative as compared with the reversible operation. It can be seen that both cells show a relatively lower degradation rate when operated in SOFC mode than in SOEC mode. The SOEC degradation rate during load cycling is rather close to the one in constant SOEC mode, and increasing the daily cycle time by reducing the

SOEC operation time from 20 hours to 8 hours seems to have minor influence. The degradation rate in SOFC mode during reversible operation is apparently higher than the one under constant condition, which may be due to the fact that the cell was degraded during the SOEC operation, thereby resulted in a lower performance in SOFC mode.

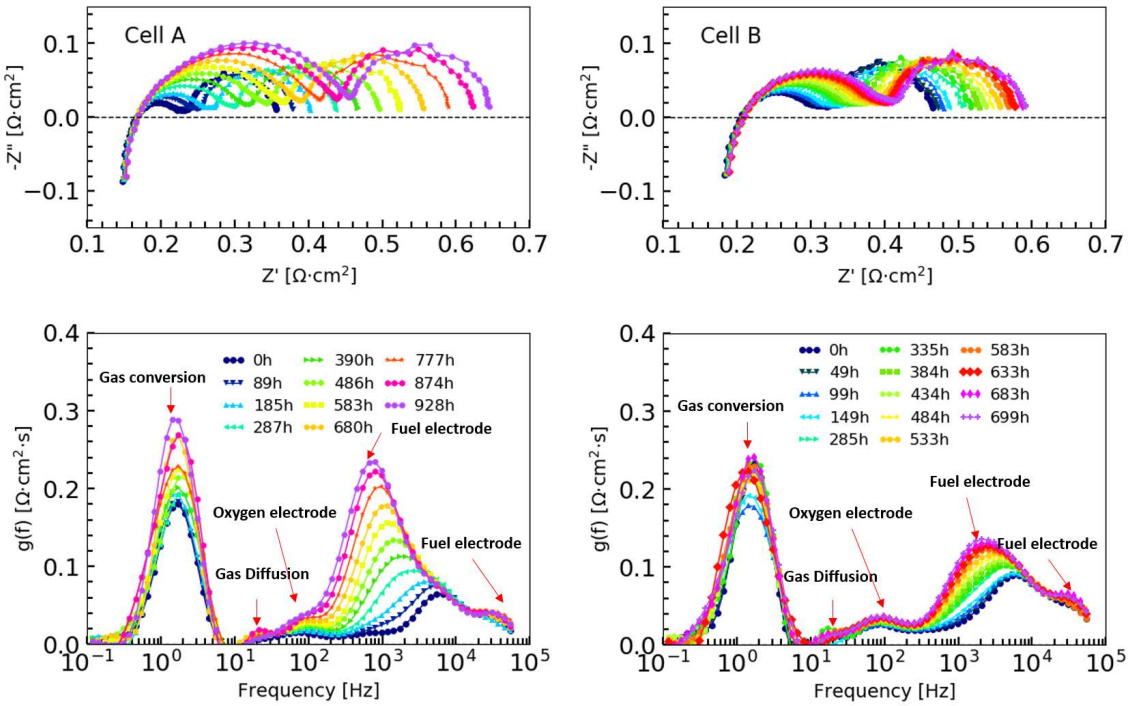

Figure 2. EIS and DRT analysis of Cell A and Cell B tested during electrolysis mode operation.

Figure 2 presents the Nyquist plots and distribution of relaxation time (DRT) analysis of the EIS measured in SOEC mode operation. The results reveals that for both Cell A and Cell B, the main degradation was due to the high frequency process with a characterization frequency range of 1 kHz to 10 kHz which has been attributed to the Ni/YSZ fuel electrode (2). On the other hand, Cell A showed a noticeable middle frequency process degradation with a summit frequency around 100 Hz, which has been reported mainly related to the oxygen electrode (2). However, the contribution to the overall degradation is minor compared to that of the fuel electrode.

Effect of operating temperature

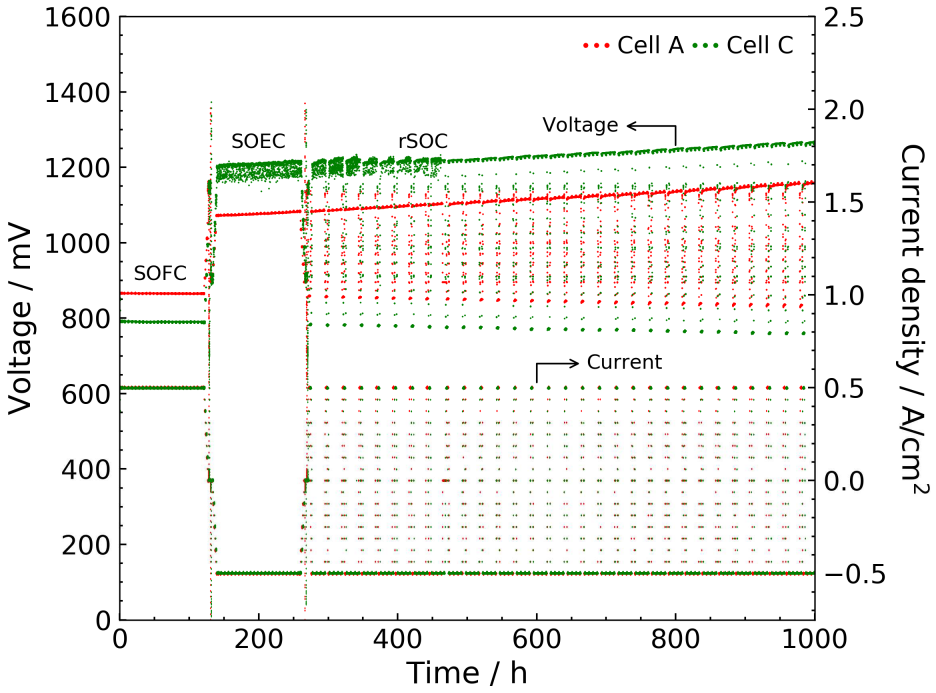

Figure 3. Effect of the operation temperature on the degradation of rSOC. Cell A was operated at 750 ˚C, while Cell C was operated at 700 ˚C

The effect of operating temperature on the cell performance is presented in Figure 3. Cell A was operated at 750 ˚C and Cell C was operated at 700 ˚C. Both cells were operated for 120h in SOFC mode and 120h in SOEC mode before changing to 3 hours SOFC operation and 20 hours SOEC operation per daily cycle of reversible operation. The degradation rates are summarized in Table III. Decreasing the operation temperature resulted in lower cell performance, i.e. higher voltage in SOEC mode and lower voltage in SOFC mode, as expected. However, the overall degradation rates seems not to be influenced by the change in temperature from 750 to 700 ˚C.

TABLE III. Cell voltage degradation rates in different operation modes. Cell A was operated at 750˚C and Cell C was operated at 700 ˚C.

Degradation rate, %/1000 h	**Constant operation**		**Reversible operation**	
	SOFC mode	**SOEC mode**	**SOFC mode**	**SOEC mode**
Cell A	0.67	8.2	3.8	10
Cell C	1.7	7.7	3.8	7

Effect of oxygen electrode configuration

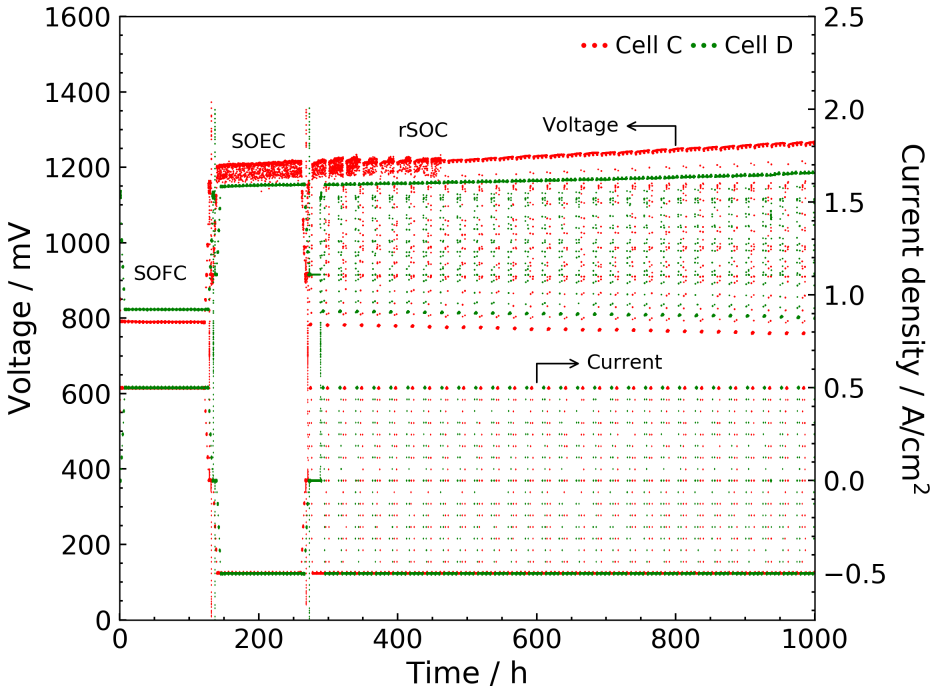

Figure 4. Effect of different oxygen electrode configurations on the cell performance. Cell C is with a LSC-CGO composite oxygen electrode and Cell D is CGO with LSC infiltrated oxygen electrode.

The effect of oxygen electrode configuration on the degradation of SOC can be seen in Figure 4. Where Cell C is type I cell with screen printed LSC-CGO composite electrode and Cell D is type II cell with LSC infiltrated CGO backbone oxygen electrode. Both cells were operated at 700 ˚C for 120 hours in SOFC mode and 120 hours in SOEC mode before changing to 3 hours SOFC and 20 hours SOEC daily cycle reversible operation. The degradation rate of the two tested cells are presented in Table IV. It can be seen that the type II cell shows better performance with lower cell voltage in SOEC mode and higher cell voltage in SOFC operation mode. Lower degradation rates is seen for Cell D (type II) than Cell C (type I). However, reversible operation seems to not have reduced the degradation in constant SOEC mode.

TABLE IV. Cell voltage degradation rate in different operation modes

Degradation rate, %/1000 h	**Constant operation**		**Reversible operation**	
	SOFC mode	**SOEC mode**	**SOFC mode**	**SOEC mode**
Cell C	1.7	7.7	3.8	7
Cell D	-1	3.7	2.5	4

Effect of reversible current density

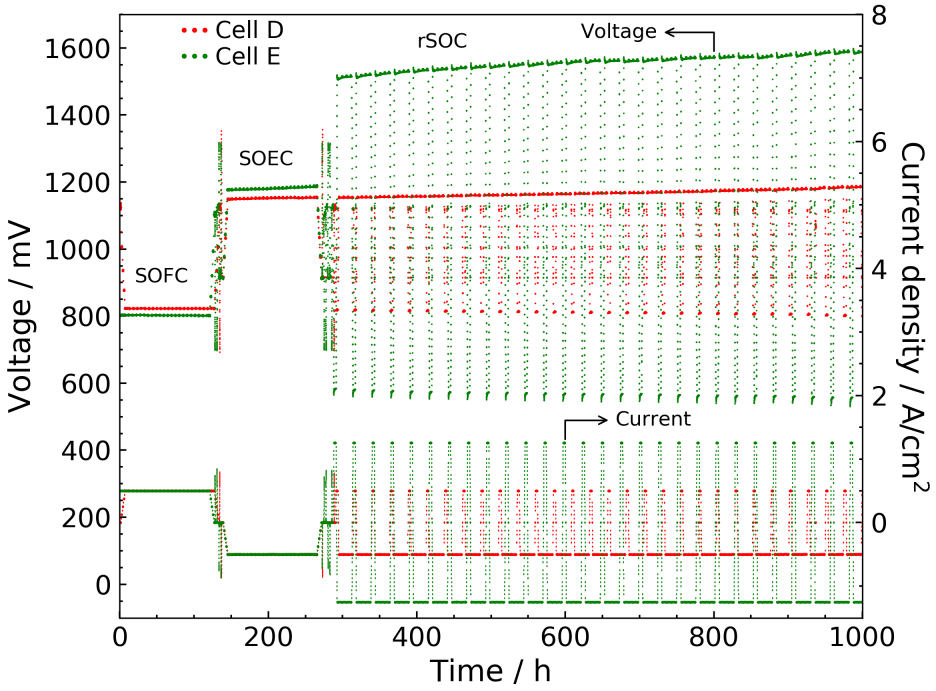

Figure 5 Effect of current density on the degradation of rSOC, Cell D was operated at ±0.5 A/cm^2 and cell E was operated at ±1.25 A/cm^2

The influence of current density on the degradation of rSOC can be seen in Figure 5. Both cells (type II) were operated for 120 hours in SOFC mode and 120 hours in SOEC mode before changing to 3 hours of SOFC and 20 hours of SOEC reversible operation. The main difference between the two cell's operation condition is that the current densities in reversible operation, where Cell D was operated at ± 0.5 A/cm^2 and cell E was operated at ± 1.25A/cm^2. The degradation rate of the two tested cells calculated based on the cell voltage are presented in Table V. The two cells showed very similar initial performance, where Cell D has slightly better performance than Cell E. The degradation show that operating the cell at ± 1.25A/cm^2 has no significant influence on the cell degradation behavior.

TABLE V. Cell voltage degradation rates in different operating modes. Cell D was operated at ±0.5A/cm^2 and Cell E was operated at ±1.25A/cm^2.

Degradation rate,	Constant operation		Reversible operation	
%/1000 h	SOFC mode	SOEC mode	SOFC mode	SOEC mode
Cell D	-1	3.7	2.5	4
Cell E	-0.1	7.4	6.7	6.3

Conclusion

In this work, five cells have been tested under different conditions to study the effect of SOFC/SOEC operating time, temperature, oxygen electrode structures and current density on the SOC degradation. Variation of initial performance is seen among the tested cells even with the same cell type, which has been identified due to the variation of contact and the electrode polarization. Nevertheless, the comparison of the long term degradation of the test results show that the cell in general has linear degradation in

SOEC mode, regardless of temperature, current density or cell type. The degradation rate in SOFC mode during reversible operation is higher than the one during constant current operation, which can be attributed to the degradation occurring during SOEC operation. The degradation of the SOC during reversible operation is dominated by the degradation taking place during SOEC operating, which most likely also affect the degradation during the SOFC part of the reversible operation. Moreover, low degradation rate can be achieved for rSOC operated at ± 1.25A/cm^2 by optimization of the oxygen electrode via infiltration of nano-electrocatalysts into the CGO backbone.

Acknowledgments

This work is supported by the project "BALANCE - Increasing penetration of renewable power, alternative fuels and grid flexibility by cross-vector electrochemical processes" under the European Union's Horizon 2020 research and innovation programme (grant agreement No. 731224).

References

1. X. Sun, M. Chen, Y.-L. Liu, P. Hjalmarsson, S. D. Ebbesen, S. H. Jensen, M. B. Mogensen, and P. V. Hendriksen, J. Electrochem. Soc., **160**, F1074 (2013).
2. P. Hjalmarsson, X. Sun, Y.-L. Liu, and M. Chen, *J. Power Sources*, **262**, 316–3 (2014).
3. S. Ovtar, X. Tong, J. J. Bentzen, K. T. S. Thydén, S. B. Simonsen, and M. Chen, *Nanoscale*, **11**, 4394 (2019).
4. G. Butera, S. H. Jensen, and L. R. Clausen, *Energy*, **166**, 738 (2019).
5. J. Mermelstein and O. Posdziech, *Fuel Cells*, **17**, 562 (2017).
6. M. Chen, J. V. T. Høgh, J. U. Nielsen, J. J. Bentzen, S. D. Ebbesen, and P. V. Hendriksen, *Fuel Cells*, **13**, 638 (2013).
7. C. Graves, S. D. Ebbesen, S. H. Jensen, S. B. Simonsen, and M. B. Mogensen, *Nat. Mater.*, **14**, 239 (2015).
8. A. Hauch, M. Marchese, A. Lanzini, and C. Graves, *J. Power Sources*, **377**, 110 (2018).
9. A. Hauch, K. Brodersen, M. Chen, and M. B. Mogensen, *Solid State Ion.*, **293**, 27 (2016).
10. http://www.soctesqa.eu/.